NACA RM A55D14

RESEARCH MEMORANDUM

THE EFFECTS OF FLEXIBILITY ON THE LONGITUDINAL AND LATERAL-DIRECTIONAL RESPONSE OF A LARGE AIRPLANE

By Henry A. Cole, Jr., Stuart C. Brown,
and Euclid C. Holleman

Ames Aeronautical Laboratory
Moffett Field, Calif.

NATIONAL ADVISORY COMMITTEE
FOR AERONAUTICS

WASHINGTON

May 27, 1955

NACA RM A55D14

NATIONAL ADVISORY COMMITTEE FOR AERONAUTICS

RESEARCH MEMORANDUM

THE EFFECTS OF FLEXIBILITY ON THE LONGITUDINAL AND LATERAL-DIRECTIONAL RESPONSE OF A LARGE AIRPLANE

By Henry A. Cole, Jr., Stuart C. Brown,
and Euclid C. Holleman

SUMMARY

Longitudinal and lateral-directional frequency responses determined from transient flight data excited by control pulses are presented for a large flexible swept-wing airplane for a wide range of flight conditions. Transient flight data are reduced to transfer-function form and comparisons are made with predicted values for the rigid and flexible airplane. Flexible-airplane transfer-function coefficients determined by the pseudostatic method show good agreement with those determined from transient flight data.

The effects of structural modes on the frequency response at various locations on the airplane are shown. These responses are compared with node lines of the calculated normal free-free modes of the airplane with particular reference to optimum location for automatic control pickups. Good correspondence is obtained between the measured frequency responses and the node lines calculated by dynamical analyses.

INTRODUCTION

In the design of an automatic control system for an airplane, the airplane response to control-surface motions should be known accurately. In the past the response has been fairly well established for relatively rigid airplanes by flight tests and theory (refs. 1 and 2). However, in recent years, the desire to increase the range and speed of large airplanes has led to sweptback wings of high aspect ratio, thin airfoils, and fuselages of high fineness ratio. All of these factors tend to increase the flexibility of the structure and the associated aeroelastic effects are becoming of greater importance in problems of static and dynamic stability and control. The dynamic effects are especially important in the design of automatic control systems because structural modes may introduce instabilities which would not arise with a rigid airplane.

Hence, it is important for the automatic control designer to consider the effects of flexibility on his control systems.

NOTATION

C_{l_α}	slope of lift curve
D	differential operator, $\frac{d}{dt}$
K_1	rolling-velocity gain
K_2	angle-of-yaw gain
K_y	radius of gyration about principal lateral axis, mean aerodynamic chords
$K_{\dot{\theta}}$	pitching-velocity gain
M	Mach number
$T_{\dot{\theta}}$	pitching-velocity time constant, sec
n	normal acceleration, positive downward, gravity units
p	rolling velocity, radians/sec
q	dynamic pressure, lb/sq ft
r	yawing velocity, radians/sec
t	time
δ_a	total aileron deflection, radians
δ_e	elevator deflection, radians
δ_r	rudder deflection, radians
$\dot{\theta}$	pitching velocity, radians/sec
ζ	damping ratio, dimensionless
ζ_a	characteristic numerator constant, dimensionless
ω	frequency, radians/sec
ω_n	undamped natural frequency, radians/sec

[redacted]

ω_a characteristic numerator constant, radians/sec

τ rolling-velocity time constant, sec

DISCUSSION

In the synthesis of an automatic control system, the aerodynamics are usually represented by a transfer function in a block diagram. As an example, the transfer functions of pitching velocity to elevator control for a rigid and a flexible airplane are presented in figure 1. The complications introduced by flexibility are apparent. Not only are the coefficients of the similar terms different from those of the rigid airplane, but also a large number of second-order terms are added to the numerator and denominator by the structural modes. These terms cannot be taken lightly because they have been directly responsible for a number of instabilities in control systems in the past (refs. 3 and 4). Also, analysis of autopilots in which control servos introduce similar terms has shown that the second-order denominator terms limit the allowable autopilot gain for stability. Fortunately, only the terms which are significant within the frequency range of the control servo need to be included. Some frequency-response data on the dynamic characteristics of the control system of a typical large airplane which may be useful in autopilot design are given in reference 5.

In order to enlarge on the experience and analytical techniques necessary to evaluate these aeroelastic effects, the NACA is flight testing a Boeing B-47 airplane over its operating range of altitudes and Mach numbers. The entire structure was instrumented with strain gages, accelerometers, and an optigraph as well as standard instruments so that the response of the complete airplane could be measured. Some of the measured acceleration frequency responses to elevator motion are shown in figure 2. The amplitude ratio is given on the upper plot and the phase angle on the lower one for a range of frequencies including the short-period mode, from 1 to 3 radians per second, and a number of structural modes, from 8 to 30 radians per second.[1] The acceleration responses at the center of gravity, wing tip, tail, and a point on the wing near the inboard nacelle are given. Several features of the response of the test airplane are apparent from these curves: (1) At frequencies below 6 radians per second, the neighborhood of the short period mode, the response is similar for all locations on the airplane and (2) at frequencies above 6 radians per second, the region of the structural modes, the response differs widely with location on the airplane and is characterized by multiple peaks in amplitude ratio and large shifts in phase

[1]Note that the amplitude ratio and frequency are plotted to logarithmic scales so that the frequency-response curves can be interpreted in terms of the characteristic forms of the transfer-function terms given in reference 6.

[redacted]

angles. The peaks correspond to the second-order denominator terms and the valleys to the second-order numerator terms in the flexible-airplane transfer functions. The part of the response below the structural modes, which is of most concern to us from a maneuvering and control standpoint, will be discussed first and the region of the structural modes later on.

Low-Frequency Response

The question is: How well can this low-frequency response be predicted? One way is to use the same form of transfer functions as for the rigid airplane, but to modify the coefficients for flexibility effects. In this method, which is called pseudostatic, the individual stability derivatives which are used to calculate the transfer-function coefficients are determined for the condition of static equilibrium between the structural spring forces and the aerodynamic loads. In addition to the usual derivatives of rigid airplanes, the lifts and moments resulting from deflections due to inertial loadings (normal acceleration and pitching acceleration) are included. These derivatives resulting from inertial loads are very important and vary widely depending on the mass distribution of the airplane. The pseudostatic method and its application to this airplane is described in detail in reference 7. Extensive work on aeroelastic effects on this airplane has also been reported in reference 8. Pitching-velocity responses predicted for pseudostatic and rigid airplanes are compared with the response measured in flight in figure 3. The agreement of experiment with the pseudostatic method is very good up to about 5 radians per second after which the structural modes dominate the response. The predicted rigid-airplane response falls considerably below the experimental response. It should be realized that accurate predictions of these responses depend a good deal on accurate estimates of the spring and mass characteristics of the airplane. In the analysis used here, the spring characteristics of the airplane were determined from static deflection measurements reported in reference 9, and the mass characteristics by ground oscillation tests which are as yet unpublished.

Longitudinal Transfer-Function Coefficients

A more comprehensive picture of the effects of flexibility over the flight range is obtained by examining the transfer-function coefficients. In figure 4, the denominator transfer-function coefficients of figure 1 are plotted versus the aeroelastic parameter, dynamic pressure multiplied by the ratio of the slopes of lift curve at the test Mach number and at zero Mach number. Also curves for 15,000 and 35,000 feet are shown so that the flight range of the airplane is pretty well covered. The solid line represents the predicted pseudostatic values and the dashed curve

the predicted rigid ones. Experimental points shown on these curves were determined from the free oscillations following pulse-elevator inputs.

The predicted values indicate a large reduction in natural frequency, ω_n, due to flexibility and this trend is well supported by the experimental points. This reduction in natural frequency is principally a result of the loss in the spring term, C_{m_α}, due to fuselage and stabilizer bending. The loss in frequency would be even greater if it were not for compensating pitching moments contributed by wing bending due to normal acceleration, a result primarily due to placing the nacelle masses near the wing tip.

As for the damping ratio, ζ, the damping and spring terms are reduced by flexibility but the compensating effects of inertial loads are such that there is little difference between the predicted rigid and pseudostatic values. The level of the experimental points is in good agreement with the predicted ones, but there is considerable scatter, probably because measurements of this coefficient are ill-conditioned when the transient motion damps out in a couple of cycles or less.

The numerator coefficients are shown in figure 5. The gain, $K_{\dot{\theta}}$, is mainly dependent on the ratio of the forcing term C_{m_δ}, to the spring term C_{m_α} for the rigid airplane. In the flexible airplane there are losses in both the forcing term and the spring term due to structural bending as well as compensating effects of inertia as mentioned in connection with the natural frequency. Hence, although there are large changes in the individual derivatives due to flexibility, it just happens in this case that the over-all effect on the gain is small. The experimental points were obtained from slow push-pull maneuvers and they agree well with the predicted ones.

The time constant, $T_{\dot{\theta}}$, is primarily the ratio of the mass to the damping force in translation and represents the phase lead of pitching velocity to angle of attack. This term is increased by flexibility because of the reduction in the damping force resulting from wing bending. The experimental points were obtained by the pulse technique and agreement with the pseudostatic values is good at 15,000 feet. At 35,000 feet the agreement is not very good which is probably due to Mach number effects which are more important than aeroelastic effects at this altitude.

Lateral Response

Similar analyses and flight-test measurements are being made for the lateral-directional response to aileron and rudder controls. Typical frequency responses (yaw damper off) obtained by the pulse technique are shown in figures 6 and 7. Also shown on these curves for comparison are

the predicted pseudostatic and rigid-airplane responses. Figure 6 presents the frequency response of rolling velocity to aileron control and figure 7 the yawing-velocity response to rudder control. The first peak in either figure represents the Dutch roll mode, and the peaks above 5 radians per second the structural modes. The aileron control excites the wing first-antisymmetrical mode primarily, and the rudder control excites the body side-bending mode. As in the longitudinal case, the response at low frequencies is similar to that of the rigid airplane for the structural modes are well separated from the Dutch roll mode. Hence, the pseudostatic approach should also apply to the low-frequency range of the lateral-directional response.

Lateral-Directional Transfer-Function Coefficients

Some preliminary values of transfer-function coefficients have been obtained by matching transient time histories from control pulses on an electronic analog. The transfer-function coefficients used for this work are shown in figure 8, and are the simplified transfer functions used for rigid airplanes. The denominator coefficients are shown in figure 9. The lateral-directional flight testing has not been completed so data are only shown for an altitude of 25,000 feet. First, consider the Dutch roll mode which is represented by the second-order denominator term in the transfer functions of figure 8. The frequency, ω_n, is lowered primarily by a loss in the spring term, C_{n_β}, due to fuselage and fin bending. The damping ratio, ζ, is also lowered primarily by fuselage and fin bending which results in a loss in damping in yaw. The time constant, τ, depends primarily on the ratio of the moment of inertia in roll to the damping in roll. While damping in roll is reduced by wing bending, the effective inertia in roll is also reduced by the rolling moments induced by wing bending under rolling acceleration loads; hence, the over-all effect is small. The experimental points show good agreement with the predicted pseudostatic values. Note that there is much less scatter in the damping ratio than for the longitudinal case because we have many cycles in the transient time histories.

The numerator terms are plotted in figure 10. The rolling-velocity gain, K_1, is decreased considerably by wing bending. Predictions indicate that this gain goes through zero at a dynamic pressure of about 720 pounds per square foot. This point, of course, is known as aileron reversal and will be approached more closely in tests at lower altitudes. The aileron reversal is most critical for outboard ailerons, which were used on this airplane (ref. 10), and for this reason there has been a trend to inboard ailerons and spoilers for lateral control of high-speed airplanes.

It may be shown that, when the flight-path angle is zero and the angle of attack is low, the terms ω_a and ζ_a are the same as ω_n and ζ,

respectively, to a first-order approximation (ref. 2). By comparison of values of ω_a and ζ_a with those of ω_n and ζ in figure 9, it may be seen that they are nearly the same when q is large. Hence, the second-order numerator term nearly cancels the Dutch roll term, and the rolling-velocity transfer function is sometimes simplified to $K_1/(1 + \tau D)$.

The numerator constant, K_2, in the yawing-velocity transfer function is primarily the forcing term, $C_{n_{\delta_r}}$, over the spring term, C_{n_β}. The tail contribution of each is reduced about the same due to fuselage and fin bending, but C_{n_β} also has a fuselage contribution, so the over-all effect of flexibility is to increase K_2. From these preliminary data, it appears that the pseudostatic method is also adequate for the prediction of low-frequency response for the lateral-directional case.

Experimental Technique

Although it is not the intention of this paper to give detailed information on the reduction of data, the reasons for the different methods used in determining experimental transfer-function coefficients should be of interest. Generally speaking, a large amount of scatter results in some of the coefficients when they are all determined from one transient record because the conditioning of the coefficients varies with the frequency content of the input. Greater accuracy is obtained if the coefficients are determined from several inputs which cover the frequency range of interest. Hence, gain constants should be determined from slow maneuvers. Denominator terms should be determined from free oscillations following inputs which excite primarily one mode at a time. When accurate values of gain and denominator coefficients are known, then the other numerator terms can be determined from the forced oscillation part of pulse control inputs. This work can either be done on an electronic analog or by curve-fitting the frequency response.

High-Frequency Response

The high-frequency part will now be examined in more detail, by referring again to figure 2. An accelerometer pickup in an automatic control system, if located at the wing tip, center of gravity, or tail, would feed voltages into the system in accordance with the high peaks and large phase shifts in the frequency responses. As mentioned before, this would be apt to compromise the stability of the system if the control servo could respond to these frequencies. However, we note that if the accelerometer were placed on the wing near the inboard nacelle where the structural-mode peaks are absent, the stability of the system would not be compromised. Optimum locations for pickups such as this can be determined from flight tests, but the question arises: How well can they be determined prior to flight?

[redacted]

In order to check this, the normal free-free modes of the complete airplane were calculated by methods similar to those in reference 11. The node lines for the first three modes are presented in figure 11. The first mode at a frequency of 8 radians per second is primarily wing first-bending mode and is called "wing flapping" by the pilots. In figure 2, it is noted that the response only peaks up near the wing tips at this frequency and that the response is small for locations on the fuselage near the node lines. The next predicted node at 23 radians per second is primarily wing first torsion. Then at a natural frequency of 27 radians per second is the body first-bending mode. It is noted that a large double peak occurs on the measured-frequency responses in the range from 20 to 30 radians per second which is undoubtedly due to the occurrence of these two modes at nearly the same frequency. Also, the peak is absent at the point where the node lines cross on the wing near the inboard nacelle. Hence, there appears to be good correspondence between the flight node lines and those predicted by dynamic analysis.

There are several other peaks in the wing-tip acceleration response besides those mentioned. Some of these are believed to be due to flexibilities in the nacelle mountings which were neglected in the analysis. Also, an additional mode appears near 16 radians per second when the short-period mode is included in the analysis (see ref. 7).

This means that the effects of flexibility can be taken entirely into account by pseudostatic methods if pickups are located on these node lines. If this is not possible, then the structural mode frequencies would either have to be filtered out or the control system tailored to be stable with their presence. It certainly would not be practical to locate all pickups and instruments at this point near the nacelle so the next best thing would be to decide which mode would affect the control system the most and to locate the pickup on the node line for that mode. For example, the high peak at 20 to 30 radians per second could also be avoided where the node lines cross the fuselage near the tail. The lines shown here are for accelerometer pickups, but lines of zero angular-velocity response can also be determined from the calculated modes for use in locating turnmeter pickups.

CONCLUDING REMARKS

In general, the pseudostatic method adequately predicts the longitudinal and lateral-directional frequency response in the region below the structural-mode frequencies. Although in some cases there were only small apparent differences between rigid and pseudostatic transfer-function coefficients, the individual aeroelastic effects on the wing and tail are large and depend a good deal on the airplane mass distribution. The agreement of experiment with pseudostatic predictions indicates that these large compensating effects are properly evaluated by the pseudostatic method.

[redacted]

The correspondence of the measured modes in flight with those calculated by dynamical analyses indicates that optimum locations for control system pickups can be determined prior to flight. When pickups are not located on these node lines, the effects of the additional second-order terms in the flexible-airplane transfer functions should be taken into account.

Ames Aeronautical Laboratory
National Advisory Committee for Aeronautics
Moffett Field, Calif., Apr. 14, 1955

REFERENCES

1. Triplett, William C., and Smith, G. Allan: Longitudinal Frequency-Response Characteristics of a 35° Swept-Wing Airplane as Determined From Flight Measurements, Including a Method for the Evaluation of Transfer Functions. NACA RM A51G27, 1951.

2. Triplett, William C., and Brown, Stuart C.: Lateral and Directional Dynamic-Response Characteristics of a 35° Swept-Wing Airplane as Determined From Flight Measurements. NACA RM A52I17, 1952.

3. White, Roland J.: Investigation of Lateral Dynamic Stability in the XB-47 Airplane. Jour. Aero. Sci., Mar. 1950, pp. 133-148.

4. Krug, Edwin H.: B-36B Autopilot Program Final Summary Report. Consolidated Vultee Aircraft Corp., Rep. FZA-36-210, Nov. 1, 1950.

5. Brown, B. Porter: Ground Tests of the Elevator Power Control System and Feel Device in a Boeing B-47A Airplane. NACA RM L54G09, 1954.

6. Lees, Sidney: Graphical Aids for Graphical Representation of Functions of the Imaginary Argument. M.I.T., Inst. Lab. Eng. Memo. E-25, Feb. 1951.

7. Cole, Henry A., Jr., Brown, Stuart C., and Holleman, Euclid C.: Experimental and Predicted Longitudinal Response Characteristics of a Large Flexible 35° Swept-Wing Airplane at an Altitude of 35,000 Feet. NACA RM A54H09, 1954.

8. Budish, Nathan N.: Longitudinal Stability at High Airspeeds. (Model XB-47) Boeing Airplane Co., Document No. D-8603, Feb. 29, 1952.

[redacted]

9. Mayo, Alton P., and Ward, John F.: Experimental Influence Coefficients for the Deflection of the Wing of a Full-Scale Swept-Wing Bomber. NACA RM L53L23, 1954.

10. Cole, Henry A., Jr., and Ganzer, Victor M.: Experimental Investigation of Rolling Performance of Straight and Swept-Back Flexible Wings With Various Ailerons. NACA TN 2563, 1951.

11. Scanlan, Robert H., and Rosenbaum, Robert: Aircraft Vibration and Flutter. The MacMillan Co., 1951.

[redacted]

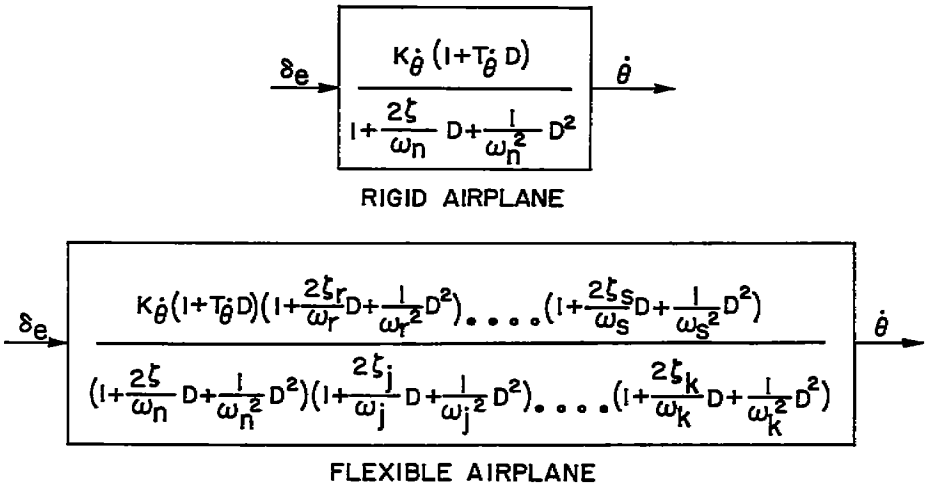

Figure 1.- Pitching-velocity transfer functions.

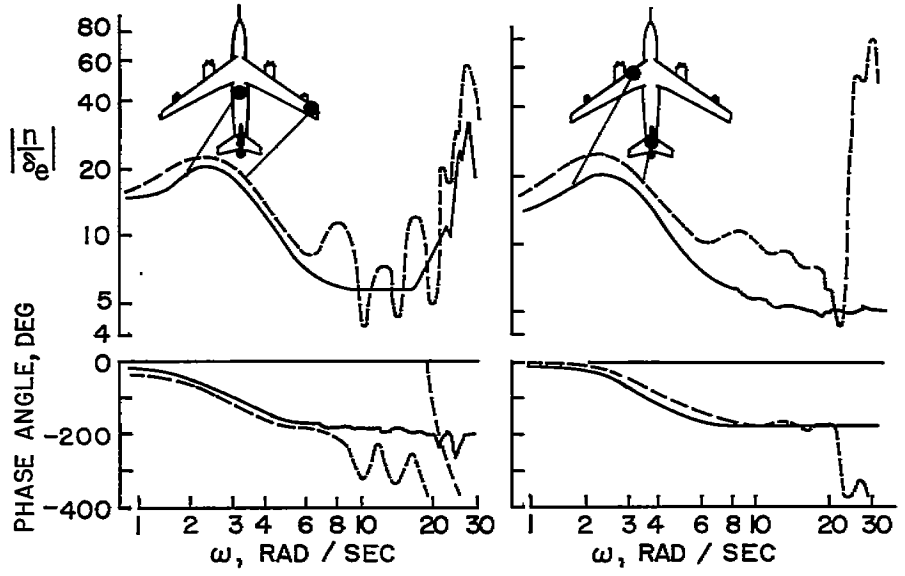

Figure 2.- Acceleration frequency response to elevator at various points; h_p = 25,000 feet, M = 0.7, c.g. = 20-percent M.A.C., W = 108,000 pounds.

[redacted]

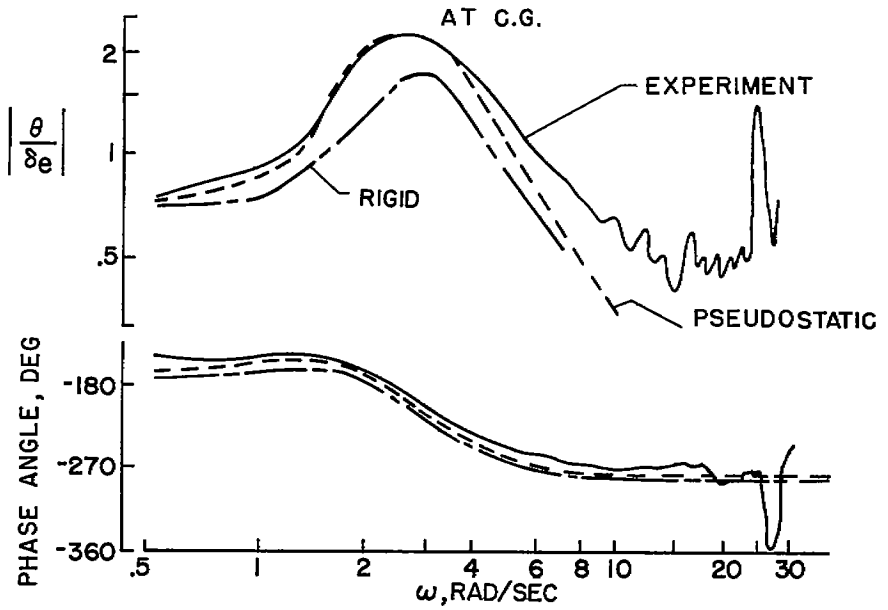

Figure 3.- Pitching-velocity frequency response to elevator at c.g.; h_p = 25,000 feet, M = 0.7, c.g. = 20-percent M.A.C., W = 108,000 pounds.

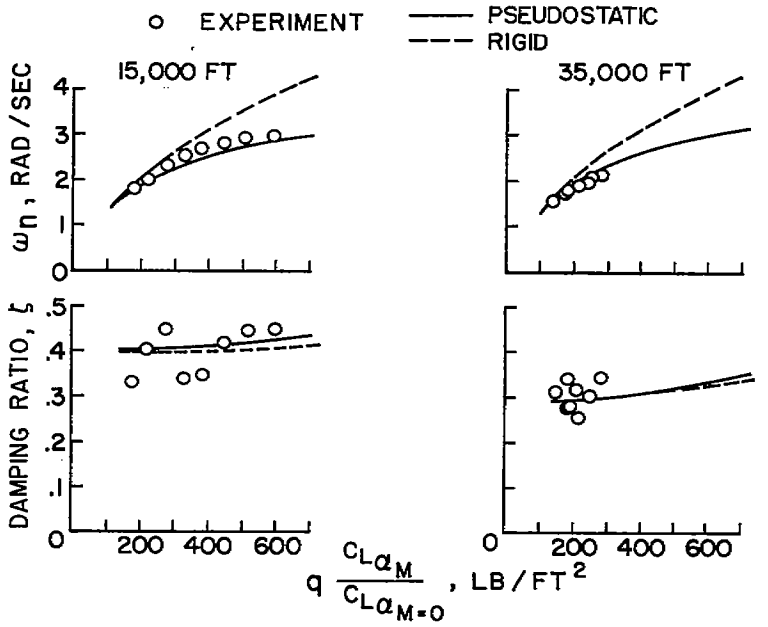

Figure 4.- Denominator coefficients of pitching-velocity transfer function; c.g. = 21-percent M.A.C., W = 115,000 pounds, K_Y^2 = 2.4.

[redacted]

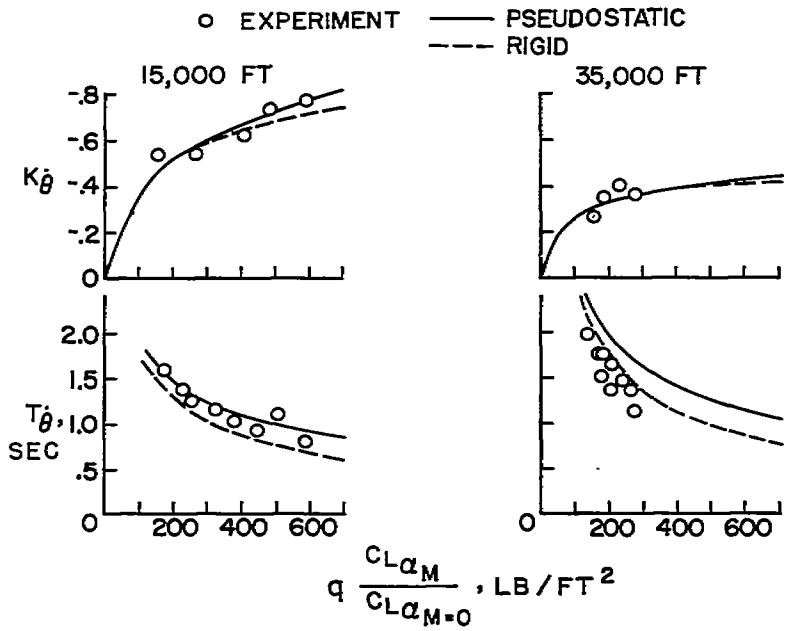

Figure 5.- Numerator coefficients of pitching-velocity transfer function; c.g. = 21-percent M.A.C., W = 115,000 pounds, K_Y^2 = 2.4.

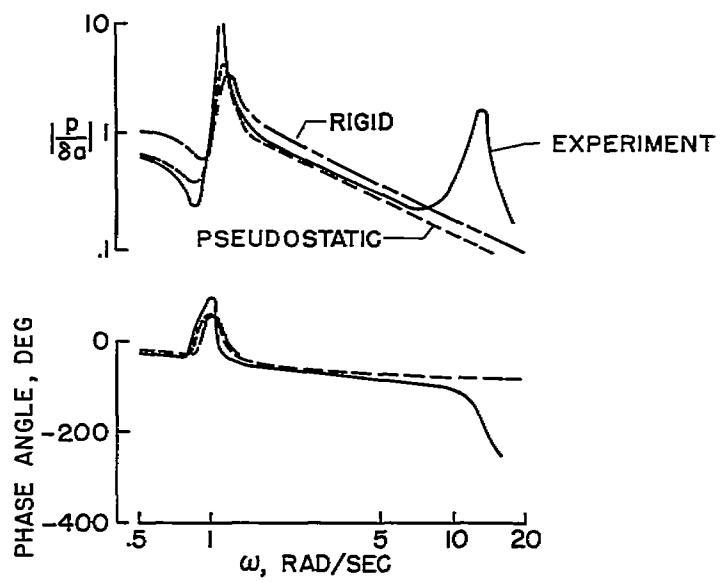

Figure 6.- Rolling-velocity frequency response to aileron at c.g.; h_p = 35,000 feet, M = 0.6, W = 117,000 pounds.

[redacted]

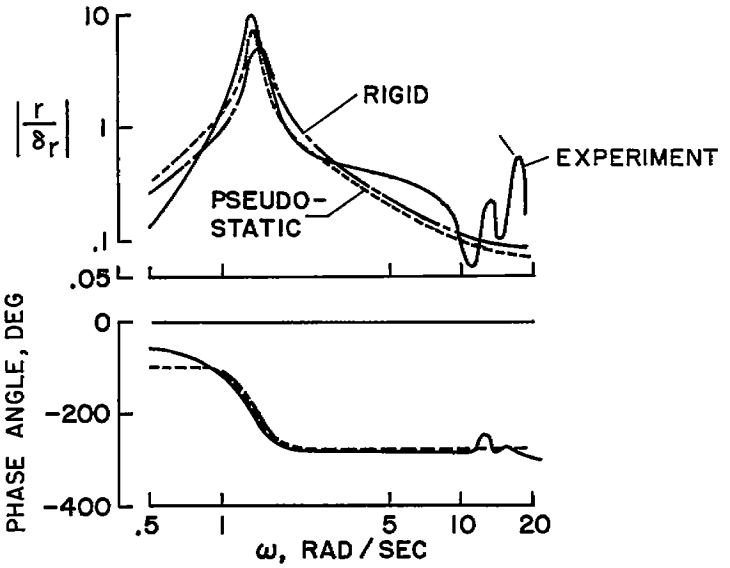

Figure 7.- Yawing-velocity frequency response to rudder at c.g.; h_p = 24,000 feet, M = 0.64, W = 104,000 pounds.

$$\delta_a \rightarrow \frac{K_1\left(1+\frac{2\zeta_a}{\omega_a}D+\frac{1}{\omega_a^2}D^2\right)}{(1+\tau D)\left(1+\frac{2\zeta}{\omega_n}D+\frac{1}{\omega_n^2}D^2\right)} \rightarrow p$$

$$\delta_r \rightarrow \frac{K_2 D}{1+\frac{2\zeta}{\omega_n}D+\frac{1}{\omega_n^2}D^2} \rightarrow r$$

Figure 8.- Lateral-directional transfer functions.

[redacted]

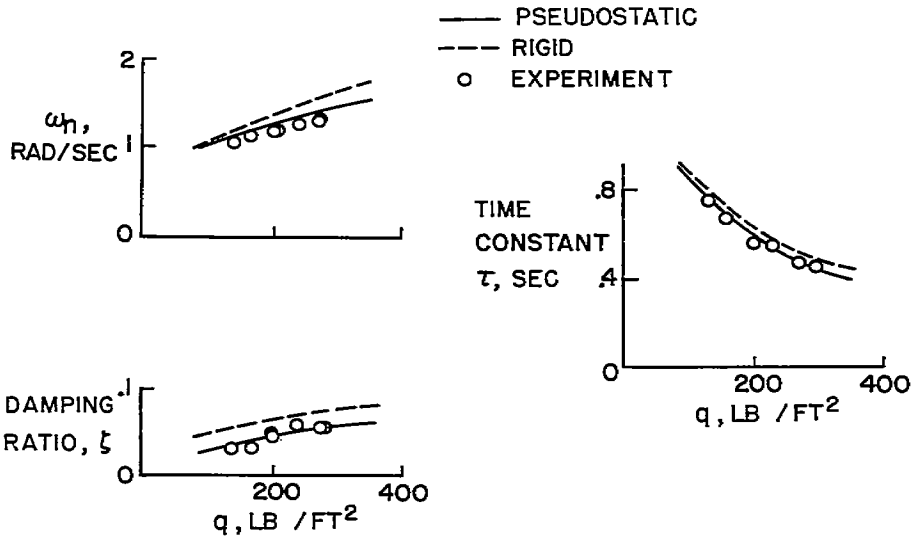

Figure 9.- Denominator coefficients of lateral-directional transfer functions; h_p = 25,000 feet, W = 115,000 pounds.

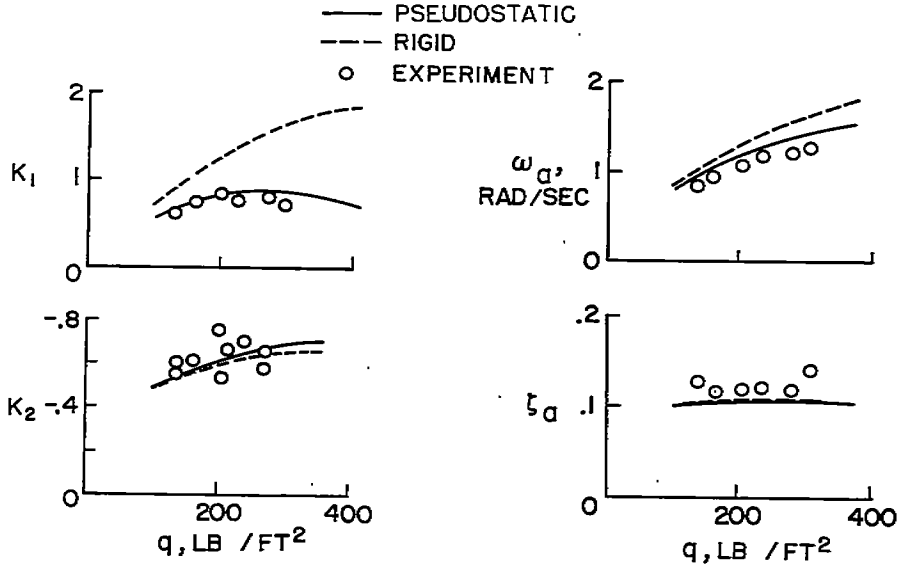

Figure 10.- Numerator coefficients of lateral-directional transfer functions; h_p = 25,000 feet, W = 115,000 pounds.

[redacted]

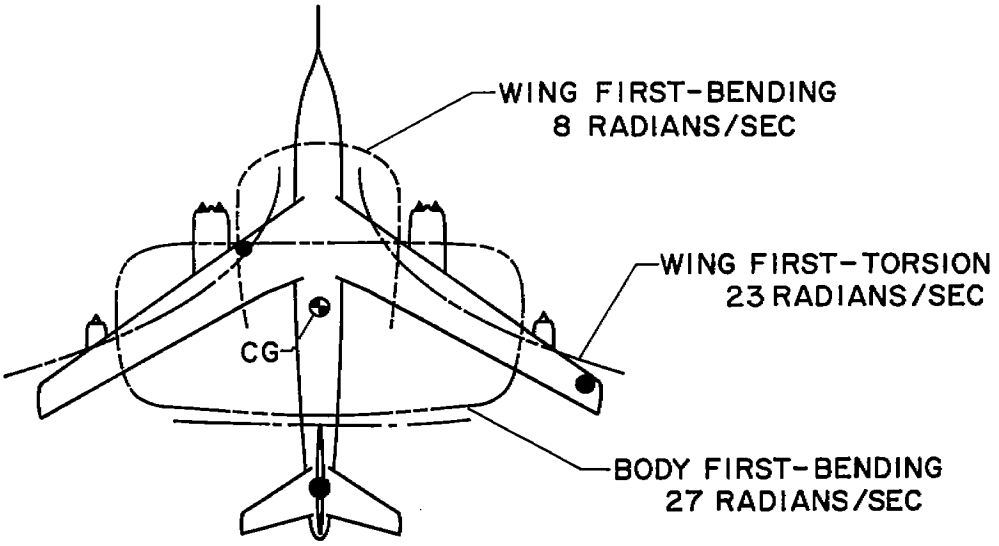

Figure 11.- Calculated longitudinal node lines.

NACA-Langley - 5-27-55 - 350